

# Design and Construction of a Dynamometer

by

Rachel E. Batzer

SUBMITTED TO THE DEPARTMENT OF MECHANICAL ENGINEERING IN  
PARTIAL FULFILLMENT OF THE REQUIREMENTS FOR THE DEGREE OF

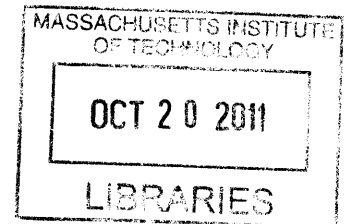
BACHELOR OF SCIENCE IN MECHANICAL ENGINEERING  
AT THE  
MASSACHUSETTS INSTITUTE OF TECHNOLOGY

JUNE 2011

© Rachel E. Batzer. All rights reserved.

The author hereby grants to MIT permission to  
reproduce and to distribute publicly paper and  
electronic copies of this thesis document in whole or in  
part in any medium now known or hereafter created.

**ARCHIVES**



Signature of Author: \_\_\_\_\_

Department of Mechanical Engineering  
May 16, 2011

Certified by: \_\_\_\_\_

Daniel Frey  
Professor of Mechanical Engineering  
Thesis Supervisor

Accepted by: \_\_\_\_\_

John H. Lienhard V  
Professor of Mechanical Engineering  
Chairman, Undergraduate Thesis Committee

# Design and Construction of a Dynamometer

by

Rachel E. Batzer

Submitted to the Department of Mechanical Engineering on  
May 16, 2011 in partial fulfillment of the requirements for the  
Degree of Bachelor of Science in Mechanical Engineering

## ABSTRACT

Access to a dynamometer is a useful tool for any electrical system where the motors must be selected from various suppliers and fully characterized. Motor suppliers usually provide a torque, speed, efficiency curve, but it frequently lacks complete motor characterization and includes motor controller losses in the total system loss. The dynamometer presented in this thesis is primarily designed for testing of high efficiency motors and motor controllers in the power and speed range requires for competition in the World Solar Challenge, a transcontinental race for solar electric vehicles. The testing specifications of a solar electric vehicles are uncommon among motor testing needs because it requires high torque, low power, high efficiency, and the only a small operating range. This thesis covers the design and construction of the dynamometer.

Thesis Supervisor: Daniel D. Frey

Title: Associate Professor of Mechanical Engineering and Engineering Systems  
co-Director, Singapore-MIT International Design Center

# TABLE OF CONTENTS

<b>1 INTRODUCTION</b> .....	<b>4</b>
1.1 SOLAR VEHICLES AND THE MIT SOLAR ELECTRIC VEHICLE TEAM .....	4
1.2 MOTIVATION .....	4
1.3 ACKNOWLEDGMENTS .....	5
<b>2 TESTING REQUIREMENTS FOR SOLAR VEHICLES</b> .....	<b>5</b>
<b>3 DYNAMOMETER DESIGN OVERVIEW</b> .....	<b>8</b>
3.1 DESIGN REQUIREMENTS .....	8
3.2 SYSTEM OVERVIEW .....	9
<b>4 MECHANICAL</b> .....	<b>10</b>
4.1 TORQUE TRANSDUCER .....	10
4.2 PLATFORM AND SHAFT CONVERTERS .....	11
4.3 SHAFT ALIGNMENT .....	12
<b>5 ELECTRICAL</b> .....	<b>13</b>
5.1 VOLTAGE MEASUREMENT .....	13
5.2 CURRENT MEASUREMENT .....	14
<b>6 LOAD MOTOR</b> .....	<b>16</b>
<b>6 TESTING</b> .....	<b>17</b>
<b>REFERENCES</b> .....	<b>20</b>
<b>APPENDIX: MECHANICAL DRAWINGS</b> .....	<b>21</b>
PLATFORM .....	22
PLATFORM: HOLE PATTERN .....	23
HUB TO SHAFT CONVERTER .....	24

# 1 INTRODUCTION

## 1.1 SOLAR VEHICLES AND THE MIT SOLAR ELECTRIC VEHICLE TEAM

The dynamometer presented here is primarily designed for the testing of motors used in solar electric vehicles. Solar vehicles use a photovoltaic array to generate electrical energy for propulsion. They almost universally utilize a battery pack to smooth power from the array and provide extra power for acceleration. Currently, solar vehicles are built purely for exhibition and competition purposes due to the low power production and high cost of solar cells. The MIT Solar Electric Vehicle Team (SEVT) is a student organization which designs, builds, and races solar vehicles. The MIT SEVT competes in the World Solar Challenge which is widely recognized as the premier solar car race in the world. The race runs from Darwin to Adelaide, a 3000 km journey across the Australian Outback (1). The electric motor is an essential part of a successful vehicle as it transforms electrical energy in mechanical propulsion. The motor specifications must be precisely matched to expected vehicle performance to maximize efficiency, minimize motor weight, and provide for the full range of speed and power requirements. Full characterization and efficiency data is an important part of optimal performance in solar racing.

## 1.2 MOTIVATION

A dynamometer is a useful tool to any racing team, but time and funding limits of the team have prevented the construction of dynamometer in the past. Recent gains in the funding of the MIT SEVT have sparked a greater need for motor data to accurately compare our motor's performance with other options. The team can also use the data to make more accurate racing strategy decisions and optimize performance for input voltage, gap adjustment, and bearing preload and selection. Availability of a dynamometer is also a good first step towards design and construction of a custom motor as the team's next major undertaking.

Unique motor requirements, intense competition, and high budgets have driven the design of super high efficiency motors which are specially built for solar racing. The current motor owned by the MIT SEVT is the NuGen Mobility SCM-150 is a 7.5 kW axial flux brushless motor which is rated at 3.75 kW continuous, weighs 20 kg, and operates at  $93\% \pm 1\%$  efficiency with controller losses in the range of racing speeds and power (2)<sup>1</sup>. The dynamometer presented here will measure both motor and motor controller losses as the previously published data about the NGM only shows the combined loss (3). Several other motor options which should have higher efficiency are available, but they are extremely

---

<sup>1</sup> NuGen Mobilty was previously named New Generation Motors and is referred to as such in the reference as the name had not changed at time of reference publication.

expensive and significant mechanical work would be required to integrate them into our vehicle. Once the power savings of an alternative motors is known, but team can determine if the funds would be best spent on a new motor or other vehicle improvements. The CSIRO motor is widely thought to be the lightest and most efficient motor available. It has a rated efficiency of 97.5% without controller losses and weighs just 10.9 kg for the stator and rotors without the motor housing (4). A 2010 paper on the CSIRO has cast some doubt on the efficiency ratings of the CSIRO and rates the CSIRO without controller at 95.5% (5) for the operating conditions of the MIT SEVT in the 2011 WSC. A dynamometer would allow the team to determine the true efficiency of the current NuGen Motor it already owns and possibly test other teams' motors in exchange for data sharing.

### **1.3 ACKNOWLEDGMENTS**

Thank you to Professor Frey for supervising this project which I brought to him from my work on the MIT SEVT.

I would like to thank who helped me with the electrical side of this project; Shane Coltan, Alex Hayman, Kelly Ran, and George Hansel. This project would not have happen without their help. I would like to give a special thanks to Alex who coaxed the motor controller into working when I was down to the wire.

The MIT SEVT has been the central pillar of my time at MIT and I am glad to have been able to contribute this project to the team.

I would also like to thank Interface Inc, Omega Engineering, and TDK Lambda who sponsored parts for this project.

## **2 TESTING REQUIREMENTS FOR SOLAR VEHICLES**

Solar vehicle have an unusual set of motor requirements because they use hub motors to prevent the loss associated with a transmission, but have much lower power requirements than a traditional vehicle. The MIT SEVT has extensive data from the previous vehicle and can make predictions about efficiency and operating range of its vehicles in future races. This information can be used to determine the range the dynamometer should be able to test. The torque transducer's accuracy is linearly related to its range because it is based on resistance through a strain gauge (6), so the dynamometer should be carefully sized to increase the accuracy of measurement. Another approach would be to size the dynamometer to the maximum motor specifications which would give more complete motor information. While this approach might be better for general applications and even allow for improved acceleration and regeneration strategy, the solar vehicle will only accelerate an average of fifteen times during the World Solar Challenge, so this energy use is inconsequential in comparison with the 60 hours of racing the vehicle will undergo.

The MIT SEVT's previous vehicle, Eleanor, average a speed of 77.6 kph and 16.1 Nm. Eleanor is a good starting point in determining the performance of future vehicles, but dynamometer specification must account for expected average speed and power use with the improvements of new and future vehicles. Racing speed, power, and torque for Eleanor from the 2009 World Solar Challenge are shown in Figures 1, 2, and 3. Only data where the vehicle maintains the same speed above 60 kph within ten percent of a five minute average are considered to eliminate anomalies such as acceleration, wind gusts, and traffic. Data points are calculated by dividing the race into five minute sections and taking the average of each section as a speed and power data point. Torque was calculated with 0.508 meter diameter wheels from the speed and power data gathered by the car's telemetry system.

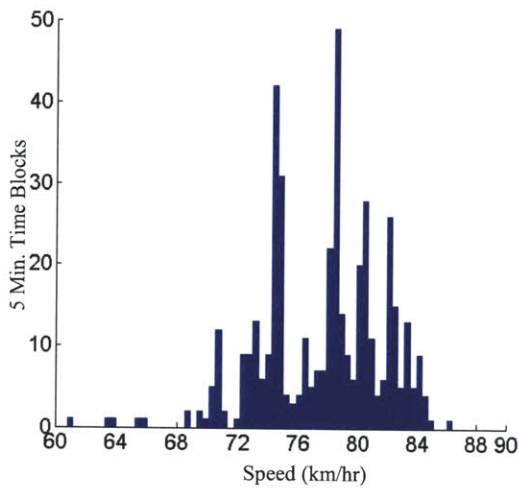


Figure 1: Histogram of Racing Speeds

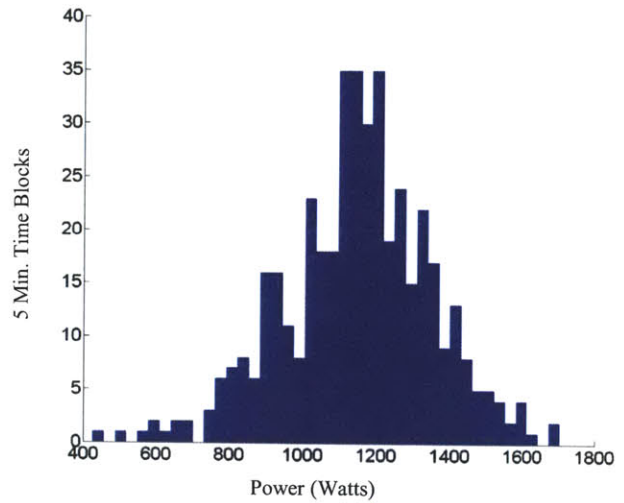


Figure 2: Histogram of Racing Power

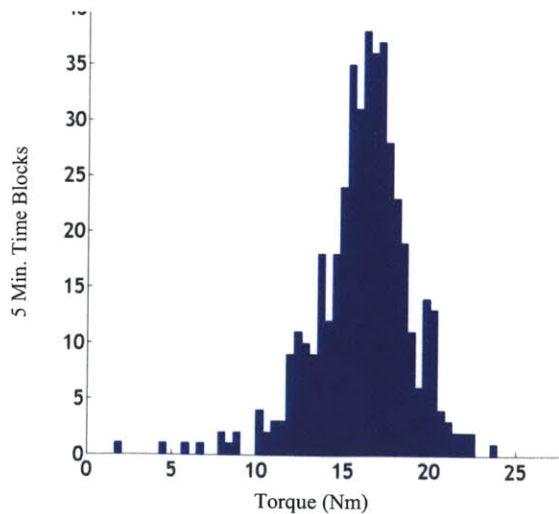


Figure 3: Histogram of Racing Torque

Assuming a similar amount of variation in speed during the next race, the dynamometer needs to be able to measure torques and speeds equal to the highest common bracket, 84 kph, modified by the efficiency improvement of the next vehicles. If strategy improves, there will be less speed variation and down time, so the maximum power dissipated will be lower. The equation below is used to calculate vehicle power consumption for a particular speed (7).

$$P_{out}(v) = \frac{\frac{1}{2} \cdot \rho \cdot C_d \cdot A \cdot v^3 + C_{rr} \cdot m \cdot v}{\eta_m * \eta_{mc}} + P_{electric} \quad 1$$

Where:

- $\rho$  = Density of Air
- $C_d$  = Coefficient of Drag
- $A$  = Frontal Area
- $v$  = Vehicle Speed
- $C_{rr}$  = Tire Rolling Resistance
- $m$  = Mass
- $\eta_m$  = Motor Efficiency
- $\eta_{mc}$  = Motor Controller Efficiency
- $P_{electric}$  = Base Electrical Loss

The race vehicle for the 2011 World Solar Challenge, Chopper del Sol, is complete and the efficiency and power production gains are known. Table 1 below details the gains made on Chopper Del Sol as a percentage and numerical change from Eleanor. Weight is reported without driver weight which is 30 kg by race regulations. Gains for vehicles beyond Chopper del Sol will be more modest, as several large improvements were implemented on Chopper which cannot be further improved in the future.

**Table 1: Design Improvements from Eleanor to Chopper Del Sol**

Category	Total Reduction	Percentage Reduction
Vehicle Mass (m)	45.3 kg	24%
Aerodynamic Drag ( $C_dA$ )	0.019 m <sup>2</sup>	17%
Motor Controller Efficiency ( $\eta_{mc}$ )	2% (estimate)	50% (estimate)
Array Power	55 Watt (increase)	5 % (increase)

By increasing power production by 5% and modifying the power consumed by the above parameters, the next vehicle should drive up to 92.7 kph for its highest speed bracket. The torque requirements are the vehicle will be reduced as speeds increase and power consumption remains relatively flat. With an increase in maximum speed of 10.4%, the torque will be proportionately decreased to a maximum sustained torque of 20.2 Nm.

### 3 DYNAMOMETER DESIGN OVERVIEW

A dynamometer is a tool for measuring power output of a motor or engine from the torque and speed of rotation. To measure the efficiency, the electrical power delivered to the motor must be measured, although this is slightly complicated by the three phase power output of the motor controller. In previously published data, the motor controller and motor efficiencies have been lumped because measurement of DC power is much simpler than three phase power.

#### 3.1 DESIGN REQUIREMENTS

The dynamometer must be designed to meet the motor and motor specifications of the MIT SEVT for current and future vehicles shown in Table 2 below. The DC voltage requirement is dictated by the maximum voltage range of the motor controller, a Tritium WaveSculptor22, which can sustain up to 160V (8). The three phase voltage, the operating voltage of the motor controller, is 96 volts for the NGM motor, but could be brought up to 160 V for the CSIRO. The current ratings are based off the lowest voltage the system will be run at and the maximum power while accounting for current sharing between phases. The DC bus of the MIT SEVT Electrical system is 108 V while the NGM motor runs at 96 V.

**Table 2: Testing Specifications**

Torque	20.2 Nm
Speed	970 RPM
Power	1600 W
DC Current	14.81 A
DC Voltage	160 V
Three Phase Current	175A max, 100 A testing
Three Phase Voltage	160V

Other major factors in the design decisions were sourcing of parts, making the dynamometer easy to use, and easy to modify for different motors. Sourcing parts was a major part of the design as the parts for power measurement can usually be easily purchased, although precision parts are expensive. The MIT SEVT is supported by corporate sponsors, so the parts which could not be built in-house were sourced based on companies who had suitable parts and were willing to donate them.



### 3.2 SYSTEM OVERVIEW

The power flow of the system starts with DC power supply from wall power. The DC power is converted to three phase by the motor controller. The test motor converts the three phase power into mechanical power which is converted back to electrical power and dissipated in the resistance of the motor's internal windings. The motor controller output can be controlled by a USB interface with a laptop to set a torque speed curve. The load motor is a series wound motor which requires an external current supply to create a magnetic field, allowing the motor constant to be changed on the fly. The current supply is controlled by the CPU. The electrical and mechanical power is measured by a custom designed electrical power monitoring system and an off the shelf torque transducer, respectively. Both of these systems output an analog signal that is converted to digital and transmitted to a laptop by a data acquisition module. This set-up will allow the dynamometer to eventually be run by closed loop control so that torque speed curves can be produced without reconstructing the data. The modules of the dynamometer are shown in Figure 4.

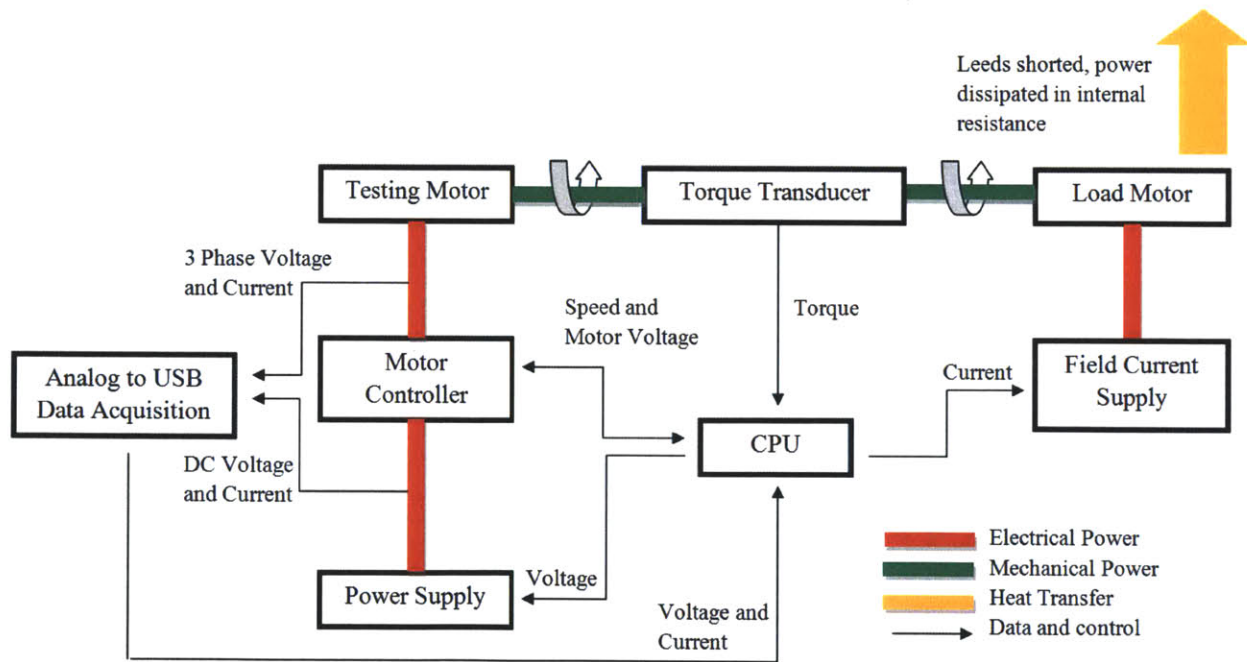
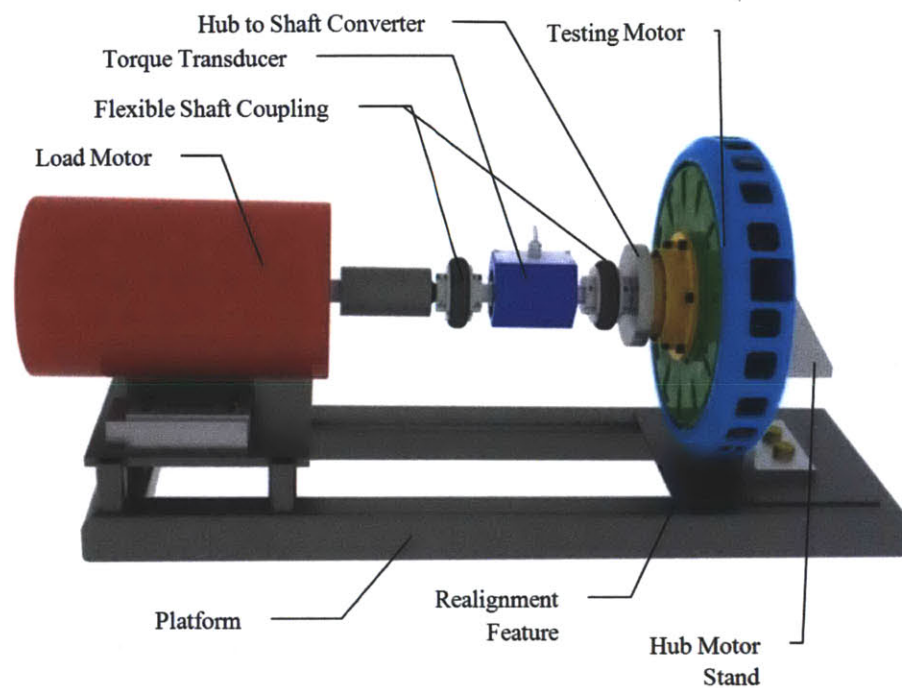


Figure 4: Dynamometer Schematic

## 4 MECHANICAL

The mechanical system was designed to be cheap and easy to manufacture while providing adjustability and precision shaft alignment. The components are pictured below in Figure 5.



**Figure 5: Mechanical Overview**

### 4.1 TORQUE TRANSDUCER

An in-line torque transducer was selected to allow direct measurement of torque on the output shaft of the motor. This type of measurement eliminates frictional losses from other components in the system and even allows the load motor to be geared without losing measurement accuracy. The torque transducer selected was a 20 Nm T8 ECO Rotary Torque Transducer which was donated by Interface Inc. Specifications of the T8 are listed in Table 3 (6).

**Table 3: T8 ECO Specifications**

Torque Measurement	0 to 20 Nm
Safe Overload Torque	36 Nm
Maximum Speed	8000 RPM
Accuracy	$\pm 0.05$ Nm
Repeatability	$\pm 0.01$ Nm
Output	$\pm 5$ V
Shaft	18 mm

The 20 Nm transducer is slightly smaller than the desired specification of 20.2 Nm, but the next largest torque range is 50 Nm. The Interface Inc. torque transducers use strain gauges to measure shaft twist which makes the measurement accuracy scale linearly with maximum measurement. The slightly decreased useful range of the 20Nm T8 was preferable to 2.5 times increase in accuracy. The  $\pm 5$  V output of the T8 is relayed to a computer with a 5 kHz USB converter supplied by Interface Inc (6).

#### **4.2 PLATFORM AND SHAFT CONVERTERS**

The platform bed and shaft converters were both designed and machined in-house. The platform was designed to house the physical size and expected torque output of the load motors to be tested. The main design goal of the platform was to make is simple to build and keep the base platforms parallel for shaft alignment. The platform was welded from mild steel square tubing to keep costs down. Once all welding process was finished, the motor mounting bases were faced without re-clamping to the mill bed to keep the bases planar. An x-y zero point was also set by machining two flats in the test motor base to allow the platform to be realigned on a mill for further machining if new mounting holes must be added. Facing of the bases and the xy zero point are pictured in Figures 6 and 7 respectively.

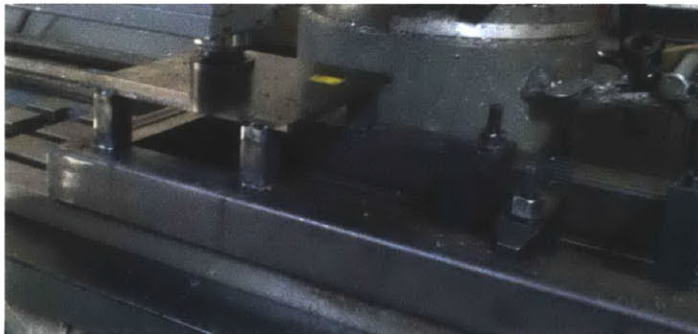


**Figure 6: Facing Platform Base**

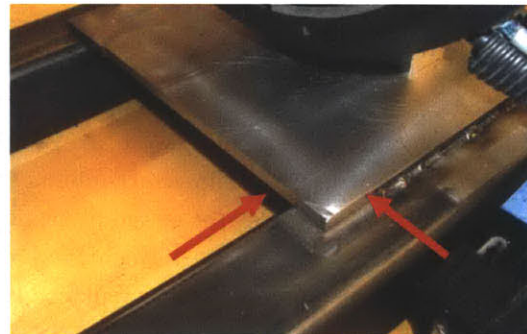


**Figure 7: X and Y Zero**

The testing motor is a hub motor, so a coupling was built to change the wheel attachment unto a shaft for connection to the torque transducer. The motor coupling was achieved via a bolted motor mount with a



concentric hole and press fit shaft. The coupling is made of 4130 steel which was chosen because of the material selection on 18 mm shafts. This coupling was machined in-house and is shown in Figure 7 at right. The MIT SEVT's suspension attachment for a previous vehicle was adapted to be the stationary mount for the load motor. It was machined from billet 6061 T6 aluminum. The stand and adapter are below in figures 8 and 9. Mechanical drawings of parts made for the dynamometer are in the Appendix.

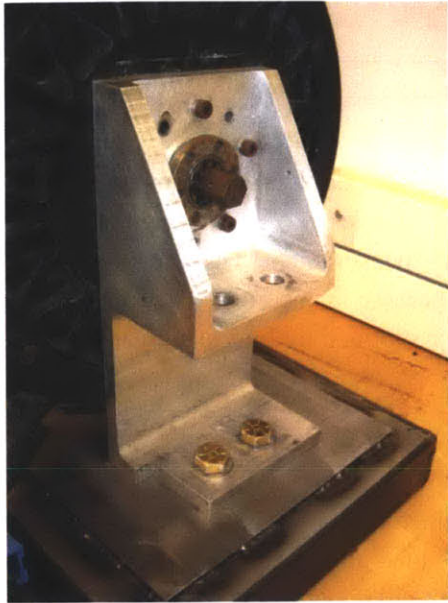


**Figure 8: Motor Stand**

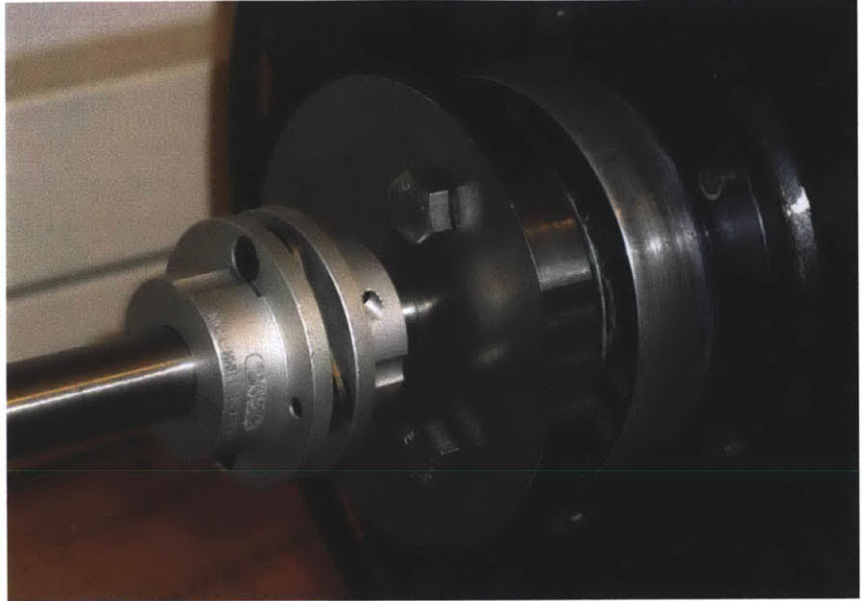


**Figure 9: Hub Motor Adapter**

### ***4.3 SHAFT ALIGNMENT***

The shafts of the torque transducer, load motor, and test motor must be carefully aligned to prevent damage to the torque transducer. Some misalignment will inevitable exist, so two single disk couplers are also added in line to absorb this misalignment. This configuration is recommended by Interface Inc (6). The couplings used are Candy Controls LK3-Single (Clamp type) couplings. Vertical alignment was and angular alignment were achieved by facing the plates in a single machining operation. The vertical offset can therefore be precisely measured by using the mill z coordinates and a spacer of the correct height was added. Horizontal alignment was achieved by connecting the shafts and then tightening down the load motor. The torque transducer was replaced with a solid shaft during this procedure to prevent excessive loads from damaging it.

## 5 ELECTRICAL

The electrical system consists of a high power DC power supply, power measurement circuitry, a high accuracy ADC with USB input, and a current supply for the load motor. The DC power supply is a Genesys™ 3.3kW donated by TDK-Lambda. It can deliver up to 150 V and 22 A. This is slightly below the optimum of 160V, but the next largest voltage was a 300 V supply which can only provide 11 A. If the complete 160 V range is required in the future, a battery pack can be used as the DC supply.

### 5.1 VOLTAGE MEASUREMENT

The electrical power is measured both before and after the motor controller to give motor and motor controller efficiency measurements. Measurement is relatively simple for the DC case because the power will be constant and referenced to ground, meaning that sample rates can be low and power can be measured with a voltage divider and current with a precision shunt. The shunt can be placed on the ground side of the power supply, meaning that the voltage across the resistor is measured with respect to ground. Measuring the three phase power is more complicated because the current measurement must float with the sinusoidal power. Furthermore, the sampling rate must be high enough to trace the sinusoid of each line or be synchronous to get instantaneous power across all three lines. High and accurate sample rates are achieved with the High Performance Multi-Function I/O USB Data Acquisition Module by Omega Engineering. The model selected is the OMB-DAQ-2416 with 16 differential or 32 single inputs at 24 bit resolution and 1 kHz (9).

Voltage measurement is performed with a simple voltage divider as diagramed at right in Figure 10 and its governing equation is shown below.

$$V_{measure} = V_0 \cdot \frac{R_2}{R_1 + R_2} \quad 2$$

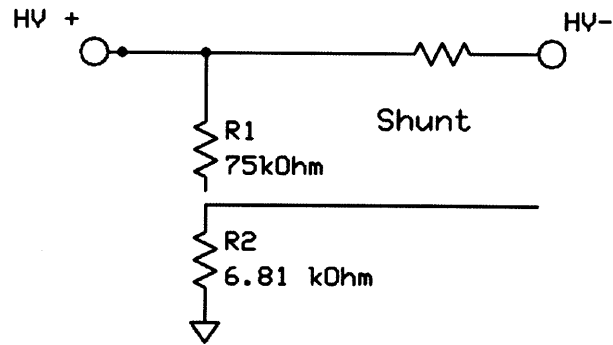


Figure 10: Voltage Divider

Resistor values were selected based on the highest expected voltage for the current system and the range of the ADC. The OMB-DAQ-2416 has 9 input ranges which can be set from  $\pm 0.078125V$  to  $\pm 20V$ . The error as a percentage of measurement is least for the highest range. Resistors which would utilize the second highest range,  $\pm 10V$ , were chosen to eliminate the possibility of over loading the DAC if the full range of the DC supply were used while increasing the error only minimally. In the initial testing cases, the voltage requirements will be 108 V and 96V. This required that the resistor ratio would need to be

10:1. The resistors selected have 0.02% value accuracy to avoid the need for calibration between resistor sets. This limits the selection of resistor values. The closest possible ratio was 75:6.81. The larger resistor is 75 kΩ to limit current flow through the divider to 1.3 mA. The voltages of the three phase lines are referenced to ground and their relative voltages are calculated after data collection for simplicity of wiring.

## 5.2 CURRENT MEASUREMENT

The current is measured across a low resistance precision shunt to produce a small voltage drop which corresponds linearly with current by the equation at right. Current measurement is simple for DC power because the shunt can be placed in line with the ground wire. This references the voltage to ground, and allows it to be fed directly to the DAC. The three phase measurement is much more difficult because each line's voltage is varying with time. The voltage across the resistor must be measured with respect to the line voltage and converted to a ground referenced voltage by an isolation amplifier. The isolation amplifier must have high accuracy, withstand 160V common mode voltage, and have a high common mode transient slew rate. Several ICs are produced for this purpose as it is common in motor control. The selected chip is the Avago Technologies HPCL-7800A Isolation Amplifier. Important specifications are presented in Table 4 (10). The gain variation is higher than desired and is therefore calibrated for each line. The amplifier outputs a differential voltage referenced to ground which is read by the DAQ. The HPCL-7800A requires a floating 5V supply which was supplied by a Texas Instruments DCR021205. The complete schematic for current measurement is shown below in Figure 11 with the physical wiring in Figure 12.

$$V = I \cdot R$$

3

**Table 4: Isolation Amplifier**

Common-Mode Rejection	15kV/μs
Gain	8.00 ± 0.08
Differential Input Operation	± 200 mV
Differential Input Suggested Operation	± 100 mV
Differential Input Limit	-2.0 V to 5.5 V

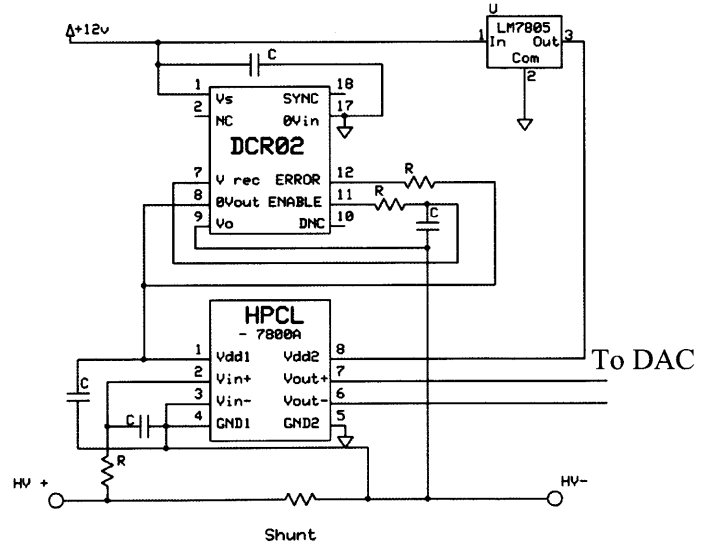


**Figure 11: Current Sense Design**

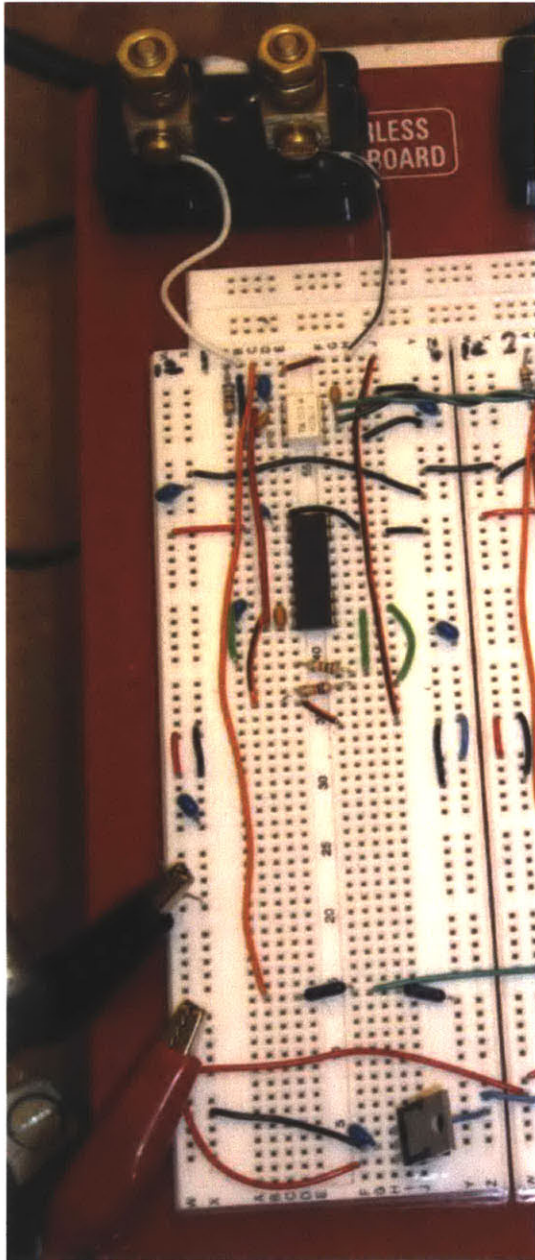


**Figure 12: Current Sense Prototype Board**

The shunt resistance determines the accuracy of measurement, with larger shunts consuming more power, but increasing accuracy. Shunt power consumption is limited to by temperature increase in the shunt which causes non-linear voltage variation and destruction of the shunt for very high currents. The shunts selected were chosen to utilize the full range of the isolation amplifiers while not over-volting the amplifier on motor start-up. The highest current the DC shunt will need to measure is 14.81 A for the maximum case. This will lead to a differential input of 148 mV. The circuit must also be able to withstand current spikes from motor start-up. This design can withstand up to 550A. Selecting the three phase shunts in more difficult. The EVC402-XXX, the motor controller being tested with the NGM, is rated to 175 A (11). Motor current is proportional to torque which is highest during heavy regenerative braking, a motor capability not tested by the dynamometer. A shunt with 0.001  $\Omega$  was selected based off motor current data from the

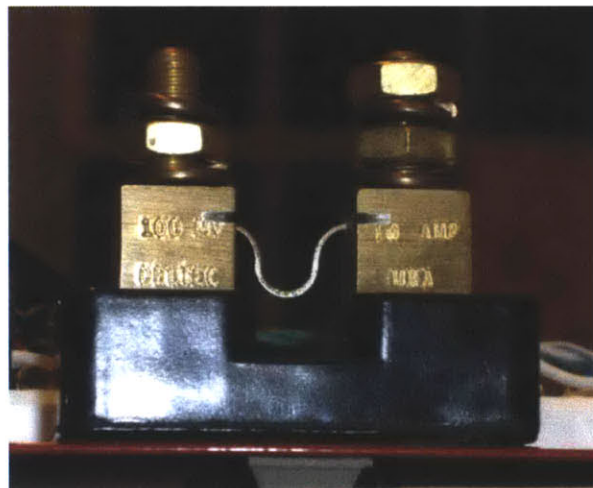


**Figure 13: Shunt**



## 6 LOAD MOTOR

The load motor needs to be able to apply a variable torque for constant speeds to simulate the loads the test motor will see during the race. This can be achieved by several methods such as connecting a DC motor in series with a power resistor bank and pulse width modulating between a larger and small resistance. A second method is to use a separately excited, or sepex, motor where the field coils are powered by an external voltage source. This allows the motor constant to be varied by changing the field strength, giving control over the torque speed curve of the motor. A D&D ES-101A-33 sepex motor was available, so this method of torque control is used. The field can be controlled by a power supply.

The dynamometer is designed for testing high torque, low speed motors, so the primary concern of the load motor is to create high enough torque in the speed range required. Figure 14 below shows the back EMF constant of the motor as a function of field voltage. Since current is linear with voltage and the back EMF constant to field voltage curve levels out at about 12 V, it is desirable to select a load resistor such that 12 V is maximum field voltage required, giving 0.13 V/rad\*s, or 0.13 Nm/A, as the maximum motor constant. The internal resistance of the motor is 0.03Ω which can be increased by adding a resistor in series or used by itself as the load by shorting the motor leads. The equations below are used to calculate the required resistive load required for a given speed and torque. Using the highest torque and lowest testing speed required, the internal resistance of the motor is a sufficient load.

$$R = \frac{\omega \cdot K_t^2}{\tau} \quad 1$$

Where:

$R$  = Internal Motor Resistance

$\omega$  = Rotational Velocity

$K_t$  = Motor Constant

$\tau$  = Torque

The load motor is set up to only supply a resistive load, but could be driven to test regenerative braking of the test motor.

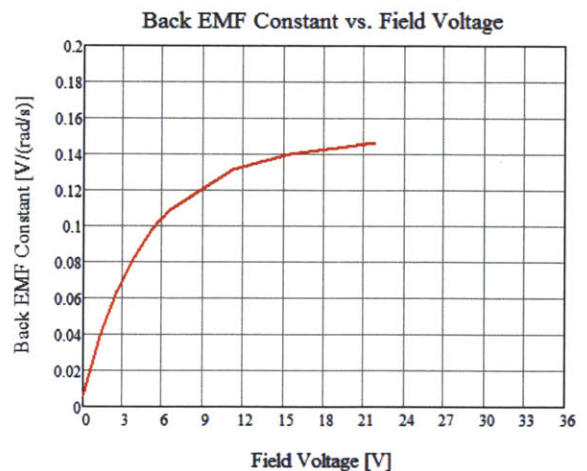


**Figure 14: Motor Constant of Load Motor**

Graph from experimental data by Shane Colton



## 6 TESTING

The torque transducer had not arrived as of the writing of this thesis, so no motor torque data could be taken. The voltage and current sense systems have been tested and are functional.

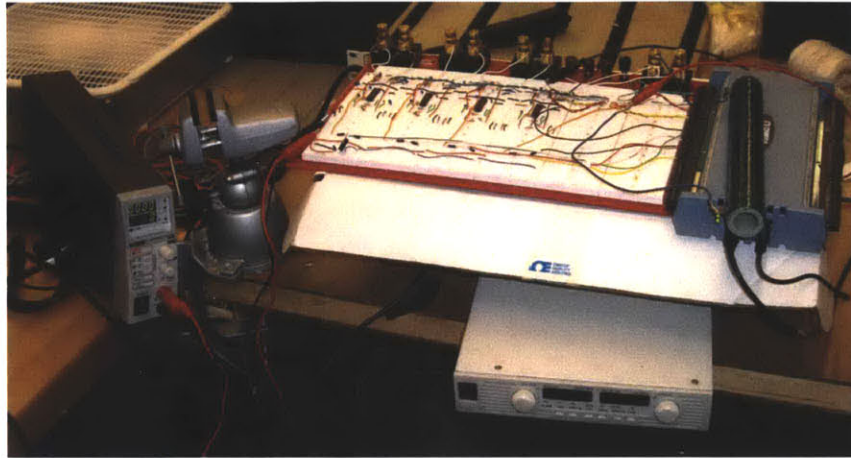


**Figure 15: Current and Voltage Board Testing**

To use the current measure system, the isolation amplifiers must be tested to determine the true gain. This is achieved by applying a current across the shunt and shorting the low load of the shunt with the board. Once this is done, the shunt voltage can be directly measured with the DAC. Voltage of the shunt and the isolation amplifier are shown as well as the error measured after calibration is done as a function of measured current for the  $0.01\Omega$  shunt.

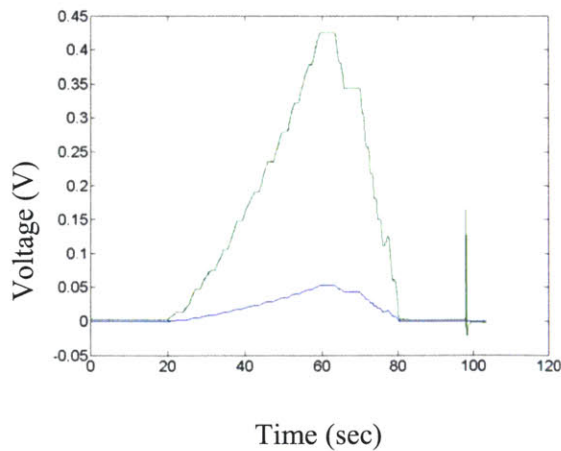


**Figure 16: Shunt and Amplifier Current**

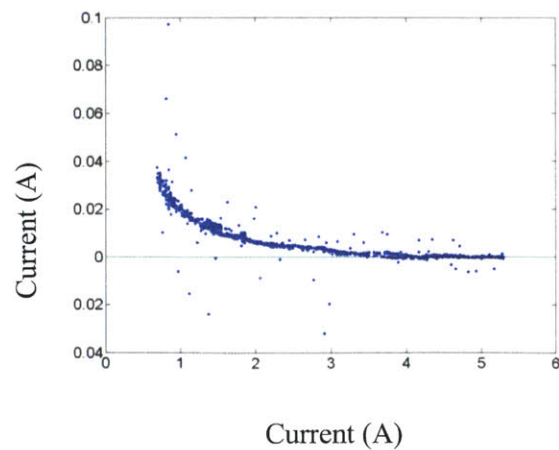


**Figure 17: Current Sense Error vs. Current**

The current and voltage sense circuitry were then added to the motor DC and phase lines to test the entire system. The test set-up is pictured below.

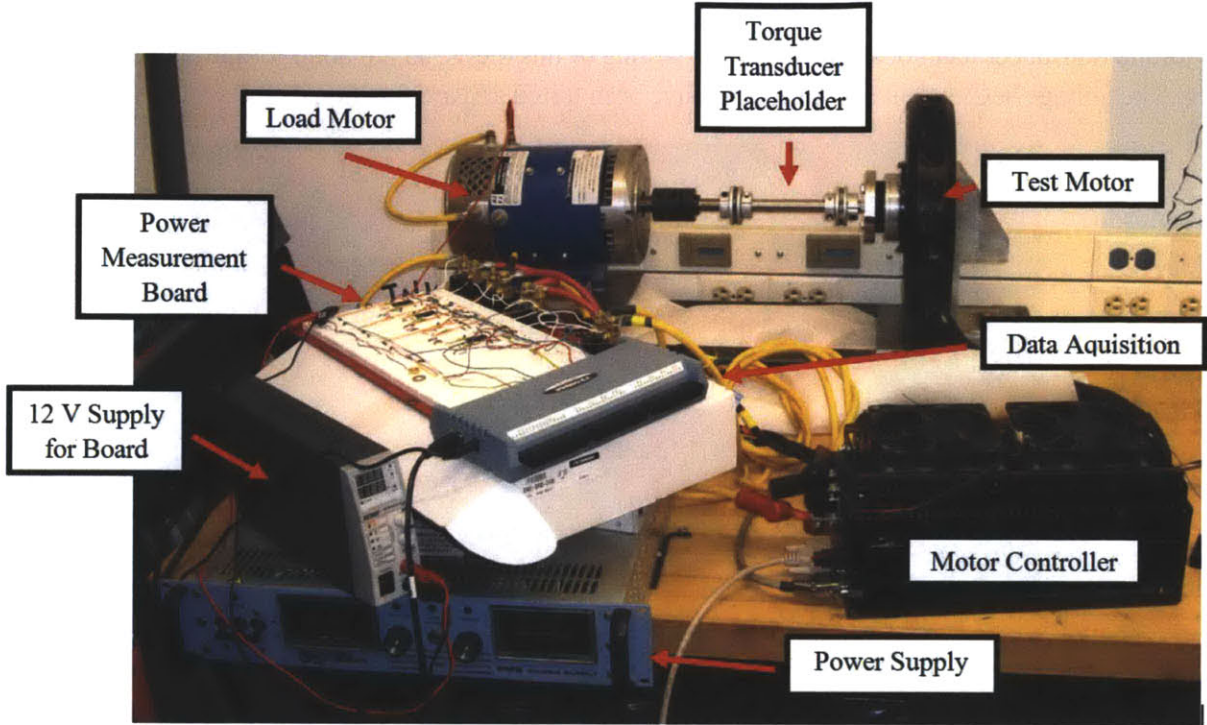


**Figure 18: Testing Set-Up**

While calculating the required sampling rate of the system, the number of poles in the motor was not accounted for. The NGM has 16 poles and the data acquisition module is limited by total number of samples per second, such that the system is only capable of sampling at a high enough rate while measuring one phase. The result of this test is shown below in Figure 19. The motor was run at 580 rpm. Red points are data points collected at 551 Hz and the sinusoidal curve was produced using the Matlab Curve Fitting Gui. The RMS current of this phase, 55.4 A, agreed with the RMS current provided by the motor controller for this test.

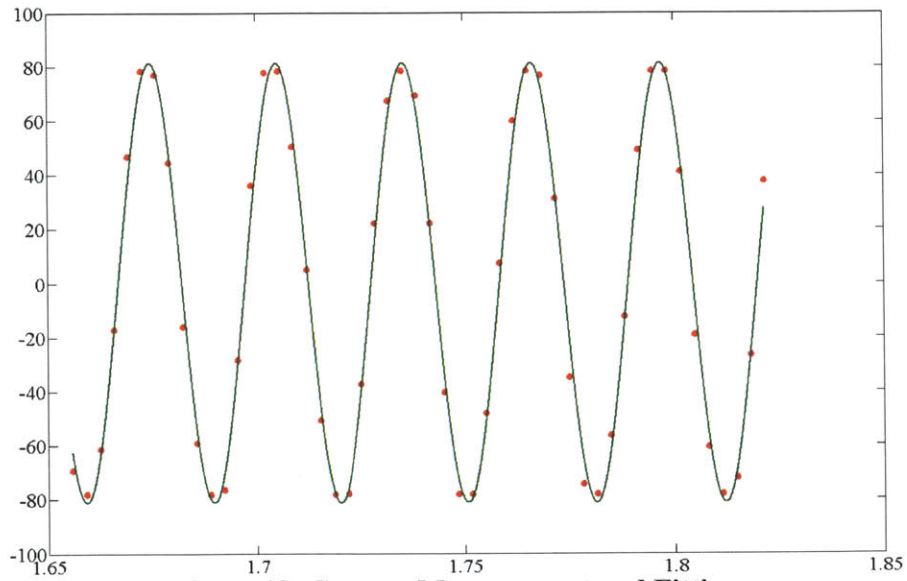


**Figure 19: Current Measurement and Fitting**

The dynamometer is shown to be functional and at least as accurate as the current sense in the EV402. It will need further work to determine the best solution to the lack of sampling frequency and to install the torque transducer when it arrives. The sampling rate issue could be solvable by assuming perfectly even power delivery by each phase or getting a faster data acquisition module.

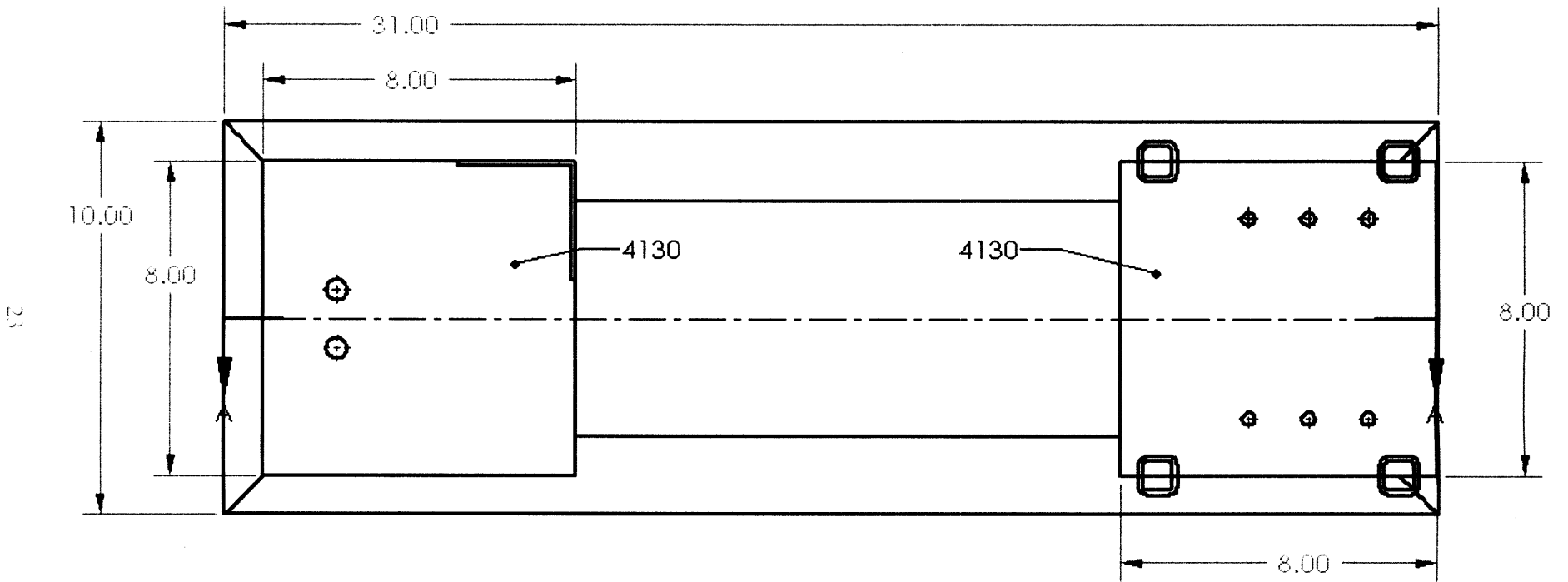
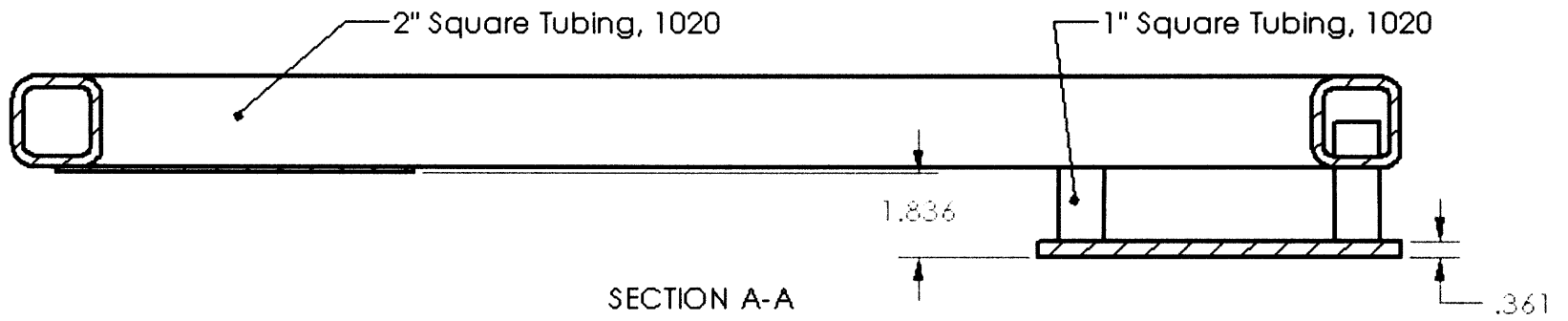
## REFERENCES

1. **World Solar Challenge.** Event Route. *World Solar Challenge*. [Online] [Cited: 5 13, 2011.] <http://www.worldsolarchallenge.org>.
2. **New Generation Motors Corporation.** SCM150-XXX Axial Flux, Brushless PM Motor. Ashburn, Virginia : New Generation Motors Corporation, 2003.
3. *Axial Flux Variable Gap Motor: Application in Vehicle Systems.* **Sung Chul Oh, Justin Kern, Ted Bohn, Aymeric Rousseau and Maxime Pasquier.** 2002-01-1088, Detroit, Michigan : SAE 2002 World Congress, 2002.
4. **H C Lovatt, V S Ramsden, and B C Mecrow.** Design of an In-Wheel Motor for a Solar-Powered Electric Vehicle. *IEEE*. Eighth International Conference on Electrical Machines and Drives, 1997, 444.
5. **Zaher, R. Al.** *Axial Flux Permanent Magnet Motor CSIRO*. s.l. : M.S. Thesis, Delft University of Technology, 2010.
6. **Interface Inc.** T8 ECO Rotary Torque Transducer. *Interface: Advanced Force Measurement*. [Online] 2011. [Cited: 5 13, 2011.] <http://www.interfaceforce.com>.
7. **Carroll, Doug.** *The Winning Solar Car*. s.l. : SAE International, 2003.
8. **Tritium Pty Ltd.** Wavesculptor22 Motor Drive. *Tritium Power Electronic Engineering*. [Online] 2011. [Cited: 5 13, 2011.] <http://www.tritium.com.au>.
9. **Omega Engineering inc.** . High Performance Multi-Function I/O USB Data Acquisition Modules. *Omega.com*. [Online] 2011. [Cited: 5 13, 2011.] <http://www.omega.com>.
10. **Avago Technologies.** HCPL-7800A Isolation Amplifier. *Avago Technologies*. [Online] 2005 - 20011. [Cited: 5 13, 2011.] <http://www.avagotech.com>.
11. **New Generation Motors Corporation.** *New EVC402-XXX 3-Phase Motor Controller*. Virginia : s.n., 2006.

## REFERENCES

1. **World Solar Challenge.** Event Route. *World Solar Challenge*. [Online] [Cited: 5 13, 2011.] <http://www.worldsolarchallenge.org>.
2. **New Generation Motors Corporation.** SCM150-XXX Axial Flux, Brushless PM Motor. Ashburn, Virginia : New Generation Motors Corporation, 2003.
3. *Axial Flux Variable Gap Motor: Application in Vehicle Systems.* **Sung Chul Oh, Justin Kern, Ted Bohn, Aymeric Rousseau and Maxime Pasquier.** 2002-01-1088, Detroit, Michigan : SAE 2002 World Congress, 2002.
4. **H C Lovatt, V S Ramsden, and B C Mecrow.** Design of an In-Wheel Motor for a Solar-Powered Electric Vehicle. *IEEE*. Eighth International Conference on Electrical Machines and Drives, 1997, 444.
5. **Zaher, R. Al.** *Axial Flux Permanent Magnet Motor CSIRO*. s.l. : M.S. Thesis, Delft University of Technology, 2010.
6. **Interface Inc.** T8 ECO Rotary Torque Transducer. *Interface: Advanced Force Measurement*. [Online] 2011. [Cited: 5 13, 2011.] <http://www.interfaceforce.com>.
7. **Carroll, Doug.** *The Winning Solar Car*. s.l. : SAE International, 2003.
8. **Tritium Pty Ltd.** Wavesculptor22 Motor Drive. *Tritium Power Electronic Engineering*. [Online] 2011. [Cited: 5 13, 2011.] <http://www.tritium.com.au>.
9. **Omega Engineering inc.** . High Performance Multi-Function I/O USB Data Acquisition Modules. *Omega.com*. [Online] 2011. [Cited: 5 13, 2011.] <http://www.omega.com>.
10. **Avago Technologies.** HCPL-7800A Isolation Amplifier. *Avago Technologies*. [Online] 2005 - 20011. [Cited: 5 13, 2011.] <http://www.avagotech.com>.
11. **New Generation Motors Corporation.** *New EVC402-XXX 3-Phase Motor Controller*. Virginia : s.n., 2006.

**APPENDIX: MECHANICAL DRAWINGS**



UNLESS OTHERWISE SPECIFIED:

DIMENSIONS ARE IN INCHES  
 TOLERANCES:  
 FRACTIONAL  $\pm 1/8$   
 TWO PLACE DECIMAL  $\pm .01$   
 THREE PLACE DECIMAL  $\pm .001$

INTERPRET GEOMETRIC  
 TOLERANCING PER:

MATERIAL  
 1020 Tubes, 4130 plate

FINISH

DO NOT SCALE DRAWING

NAME DATE

DRAWN  
 CHECKED  
 ENG APPR.  
 MFG APPR.

Q.A.

COMMENTS: Only important  
 dimensions called out.  
 Hole pattern in  
 Platform: Hole Pattern

TITLE:

Platform

SIZE DWG. NO.

**A** base2

REV

SCALE: 1:4 WEIGHT:

SHEET 1 OF 1

**PROPRIETARY AND CONFIDENTIAL**  
 THE INFORMATION CONTAINED IN THIS  
 DRAWING IS THE SOLE PROPERTY OF  
 <INSERT COMPANY NAME HERE>. ANY  
 REPRODUCTION IN PART OR AS A WHOLE  
 WITHOUT THE WRITTEN PERMISSION OF  
 <INSERT COMPANY NAME HERE> IS  
 PROHIBITED.

NEXT ASSY

USED ON

APPLICATION

5

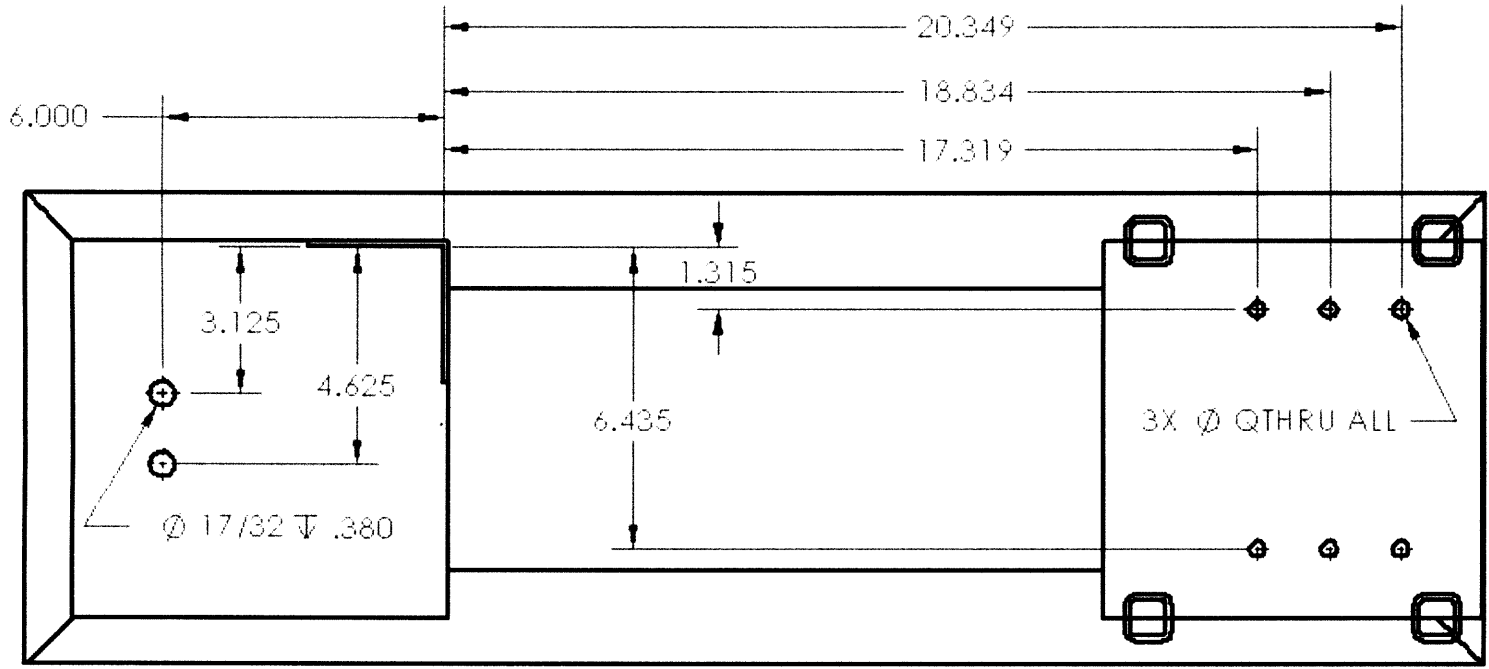
4

3

2

1





24

**PROPRIETARY AND CONFIDENTIAL**  
 THE INFORMATION CONTAINED IN THIS DRAWING IS THE SOLE PROPERTY OF <INSERT COMPANY NAME HERE>. ANY REPRODUCTION IN PART OR AS A WHOLE WITHOUT THE WRITTEN PERMISSION OF <INSERT COMPANY NAME HERE> IS PROHIBITED.

NEXT ASSY USED ON

APPLICATION

UNLESS OTHERWISE SPECIFIED:

DIMENSIONS ARE IN INCHES  
 TOLERANCES:  
 FRACTIONAL  $\pm 1/8$   
 TWO PLACE DECIMAL  $\pm .01$   
 THREE PLACE DECIMAL  $\pm .001$

INTERPRET GEOMETRIC TOLERANCING PER:  
 MATERIAL  
 1020 Tubes, 4130 plate

FINISH

DO NOT SCALE DRAWING

NAME DATE

DRAWN  
 CHECKED  
 ENG APPR.  
 MFG APPR.  
 Q.A.  
 COMMENTS:

TITLE:

Platform:  
 Hole Pattern

SIZE DWG. NO.

REV

**A** base

SCALE: 1:8 WEIGHT:

SHEET 1 OF 1

5

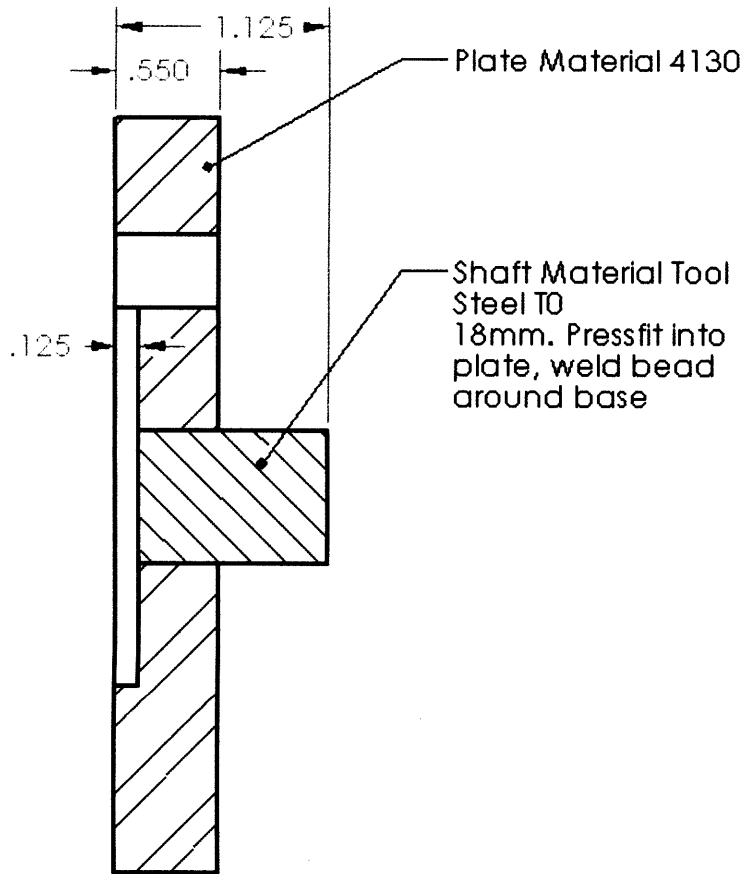
4

3

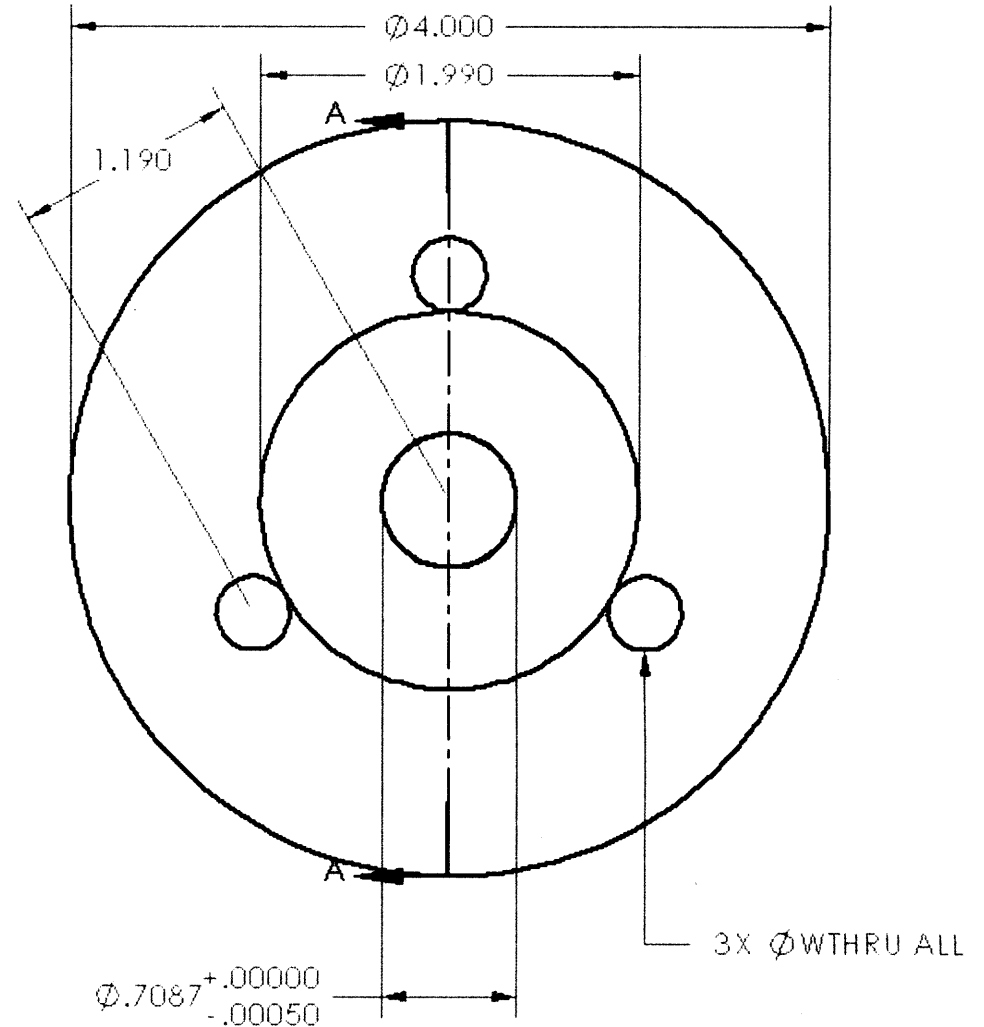
2

1





SECTION A-A



25

UNLESS OTHERWISE SPECIFIED:

DIMENSIONS ARE IN INCHES  
TOLERANCES:  
FRACTIONAL ±  
ANGULAR: MAX CH ± BEND ±  
TWO PLACE DECIMAL ± .01  
THREE PLACE DECIMAL ± .005

INTERPRET GEOMETRIC  
TOLERANCING PER:  
MATERIAL

FINISH

DO NOT SCALE DRAWING

NAME DATE

DRAWN

CHECKED

ENG APPR.

MFG APPR.

Q.A.

COMMENTS:

TITLE:

Hub to Shaft  
Converter

SIZE DWG. NO.

**A** hubtoshaft 1

SCALE: 1:1 WEIGHT:

SHEET 1 OF 1

PROPRIETARY AND CONFIDENTIAL  
THE INFORMATION CONTAINED IN THIS  
DRAWING IS THE SOLE PROPERTY OF  
<INSERT COMPANY NAME HERE>. ANY  
REPRODUCTION IN PART OR AS A WHOLE  
WITHOUT THE WRITTEN PERMISSION OF  
<INSERT COMPANY NAME HERE> IS  
PROHIBITED.

NEXT ASSY

USED ON

APPLICATION

5

4

3

2

1